J Nanostruct 16(1): 756-765, Winter 2026

RESEARCH PAPER

# Novel Approach to Magnetic Core-Shell Nanostructures of ZnAl Layered Double Hydroxide for Controlled Drug Release of Ciprofloxacin

*Sorour Bakhshi Sichani, Mohammadreza Mansournia**

*Department of Inorganic Chemistry, Faculty of Chemistry, University of Kashan, Kashan, I. R. Iran*

**ARTICLE INFO**

***Article History:***
*Received 27 September 2025*
*Accepted 25 December 2025*
*Published 01 January 2026*

***Keywords:***
*Ciprofloxacin*
*Drug release*
*Layered double hydroxide*
*Nanohybrid*

**ABSTRACT**

This research exhibits a novel approach to constructing the ZnAl layered double hydroxide (ZnAl-LDH) as a shell on the core of $Fe_3O_4$ nanoparticles, followed by the intercalation process of an antibiotic drug, ciprofloxacin (cip). Also, the advantages of the synthetic $Fe_3O_4$@ZnAl-LDH as a delivery agent model are investigated. The obtained biocompatible nanostructures were characterized by a range of techniques such as FT-IR, XRD, EDX, FE-SEM, and TGA. Based on the X-ray diffraction results, the increase in the interlayer space indicated successfully intercalation of cip (ZnAl-LDH-cip 95.87 % and $Fe_3O_4$@ZnAl-LDH-cip 94.48 %,). The surface morphology, examined by the scanning electron microscopy imaging, displayed the stacked sheets of LDH. In addition, the drug release properties, studied in PBS buffer (pH=7.4) at 37 °C, illustrated a sustained release profile. The great rates of 81.27 % and 82.43 %, were found after 24 h for ZnAl-LDH-cip and $Fe_3O_4$@ZnAl-LDH-cip, respectively. The studies showed that the as-synthesized $Fe_3O_4$@ZnAl-LDH can be used as an efficient nanocarrier in the targeted and controlled drug release systems.

**How to cite this article**
*Sichani S., Mansournia M. Novel Approach to Magnetic Core-Shell Nanostructures of ZnAl Layered Double Hydroxide for Controlled Drug Release of Ciprofloxacin. J Nanostruct, 2026; 16(1):756-765. DOI: 10.22052/JNS.2026.01.068*

## INTRODUCTION

Nowadays, nano has made great progress in drug delivery, reduction of side effects of drugs, early diagnosis of diseases, and treatment of incurable diseases [1, 2]. Organic and inorganic nanoparticles can also be used in drug delivery systems, which have been of great interest in recent years [3–6]. Layered or two-dimensional composites whose crystal structures are formed by the juxtaposition of two-dimensional units by weak forces, have engrossed the consideration of scientific communities due to their high potential in industrial usage, controllability, and the possibility of partial deformation in the interlayer space. The basic structure of layered double hydroxides, indicated by the abbreviation LDH, is based on the structure of brucite Mg(OH) with the characteristic of anion exchange. In such structure, cations are placed inside the layers and anions along with water molecules are placed between the layers. The general formula of LDHs is $[M^{II}_{1-x}M^{III}_{x}(OH)_2]^{x+}[A^{n-}_{x/n}]^{x-}.mH_2O$, where the practical importance of them is due to the high charge density of their layers [7–9]. Also, easy, cheap and changeable synthesis, and renewable source have attracted a lot of attention to the use of these compounds. Positively charged LDHs as the host compounds for the synthesis of organic-mineral nanolayers

* *Corresponding Author Email: Mansournia@kashanu.ac.ir*

can place negatively charged biomolecules between their layers [10]. The high ability of these layered structures to exchange anions has caused applications of these compounds in various fields such as pollutant absorbers [11], catalysts [12, 13], ion exchangers [14, 15], drug carriers [16–18], electrochemistry [19–21], and reinforcing agents in polymer materials [22].

Delivering the drug to the desired tissue causes accumulation and thus increases the activity of the drug, and on the other hand, minimizes the toxicity of the drug on other tissues, which is defined as a targeted release. In addition, the carriers have led to improved stability and solubility of drugs [23, 24]. Recently, LDH-based drug delivery systems have been reported for ciprofloxacin (cip), which is effective in the treatment of various microbial infections [25, 26]. On the other hand, the cores in core-shell nanostructures can be made from various materials with different sizes, shapes, and properties. In the meantime, magnetite nanoparticles as the most important category of magnetic particles have received very consideration due to their great characteristics; ideal size and suitable biocompatibility. [27–30]. In this research, a new approach is utilized for the synthesis of Zn-Al layered double hydroxide nanostructures using an ammonia atmosphere. Since the ability to control the drug carrier by the external magnetic field improves its targeting and reduces its possible side effects in the patient's body, the synthesis of a delivery system with the core-shell structure consisting of a magnetic core is also carried out. Further, the potential of the as-obtained nanostructures for the loading and then releasing of ciprofloxacin drug are investigated.

## MATERIALS AND METHODS

### *Raw materials*

The metal salts of $FeSO_4.7H_2O$, $Zn(NO_3)_2.6H_2O$, $Al(NO_3)_3.9H_2O$, $Na_2HPO_4$, $KH_2PO_4$, KCl, and NaOH were purchased from Merck, and ciprofloxacin were obtained from Sigma-Aldrich. Ammonium hydroxide 25 %, hydrochloric acid 37 %, and absolute ethanol were also procured from Merck Company. All the chemicals were of analytical grade and used without any further purification. Phosphate buffered saline (PBS) solution was prepared using $Na_2HPO_4$ (2.40 gr), $KH_2PO_4$ (0.40 gr), and KCl (0.03 gr) per liter deionized water. The pH was adjusted to 7.4 by hydrochloric acid or sodium hydroxide 1 M at 37 °C.

### *Preparation of $Fe_3O_4$ core*

The magnetite nanoparticles were synthesized via a hydrothermal method based on our previous procedure [31]. Briefly, two beakers one of them containing 0.139 gr $FeSO_4.7H_2O$ dissolved in 10 ml distilled water and another one comprising 10 ml of the ammonia solution were transferred into an autoclave (with a capacity of 300 ml), beside each other. The autoclave was heated at 75 °C for 1h. Then, the black precipitate was collected and washed with distilled water and ethanol several times and dried at 75 °C.

### *Preparation of ZnAl-LDH and ZnAl-LDH-cip*

The ZnAl-$NO_3$ LDH was synthesized using the above hydrothermal method at the ammonia atmosphere similar to that of $Fe_3O_4$ preparation. Initially, 10 ml of an aqueous solution including $Zn(NO_3)_2.6H_2O$ (0.01 M) and $Al(NO_3)_3.9H_2O$ (0.005 M), with the Zn/Al molar ratio of 2:1 under vigorous stirring in a beaker along with another beaker containing 10 ml of ammonia solution were put in an autoclave at room temperature for 1h. The product was separated by centrifugation and was washed several times with distilled water and ethanol, respectively, then was dried at 75 °C for 12 h. For the intercalation of the drug into the interlayer space of ZnAl-LDH, cip (0.017 gr) was also dissolved in the initial solution in addition to the $Zn^{2+}$ and $Al^{3+}$ nitrate salts. In this regard, the mole ratio of drug/Al in the preparation of ZnAl-LDH-cip was 1:1.

### *Preparation of $Fe_3O_4$@ZnAl-LDH-cip*

In order to coat the magnetite cores with the drug loaded nanocomposites, ZnAl-LDH-cip, 0.002 gr of the as-made $Fe_3O_4$ was ultrasound dispersed in the solution of 0.017 gr of cip, 0.026 gr $Zn(NO_3).6H_2O$ and 0.018 gr of $Al(NO_3).9H_2O$ in 10 ml distilled water for 30 min. The obtained mixture was placed in an autoclave, beside the beaker of 10 ml $NH_3$ solution. After standing at room temperature for 1h, the brown precipitate was collected by centrifugation, rinsed several times with distilled water and ethanol to remove the impurities, and finally dried at 75 °C.

### *Instruments*

The crystal structure of the products was recognized using X-ray diffraction (XRD) by a Philips X'pert pro diffractometer with graphite mono achromatized Cu ka radiation having λ =

1.5406 Å. FT-IR spectra were recorded using a Magna 550 Nicolet spectrometer and the KBr pellets in the wavenumber region of 400-4000 $cm^{-1}$. Furthermore, a field emission scanning electron microscope (FE-SEM), TESCAN Mira3, coupled to energy-dispersive X-ray spectrometer (EDX) was utilized in order to investigate the morphological and elemental composition of the as-made samples. The thermogravimetric analysis (TGA) was carried out using a STA530 instrument with heating temperature from 0 to 900 ˚C under an argon atmosphere. The amount of drug loaded on the as-made LDH carriers and released from them were estimated by employing a single beam UV-Vis spectrometer (Advanced spectroscopy CO. IRAN) in the wavelength range of 200-900 nm using a quartz cell.

*Drug loading capacity*

The amount of ciprofloxacin entrapped into the layered double hydroxide was evaluated as follows: During the centrifugation step in the preparation of $Fe_3O_4$@ZnAl-LDH-cip, the supernatant was collected and its absorbance was measured at the

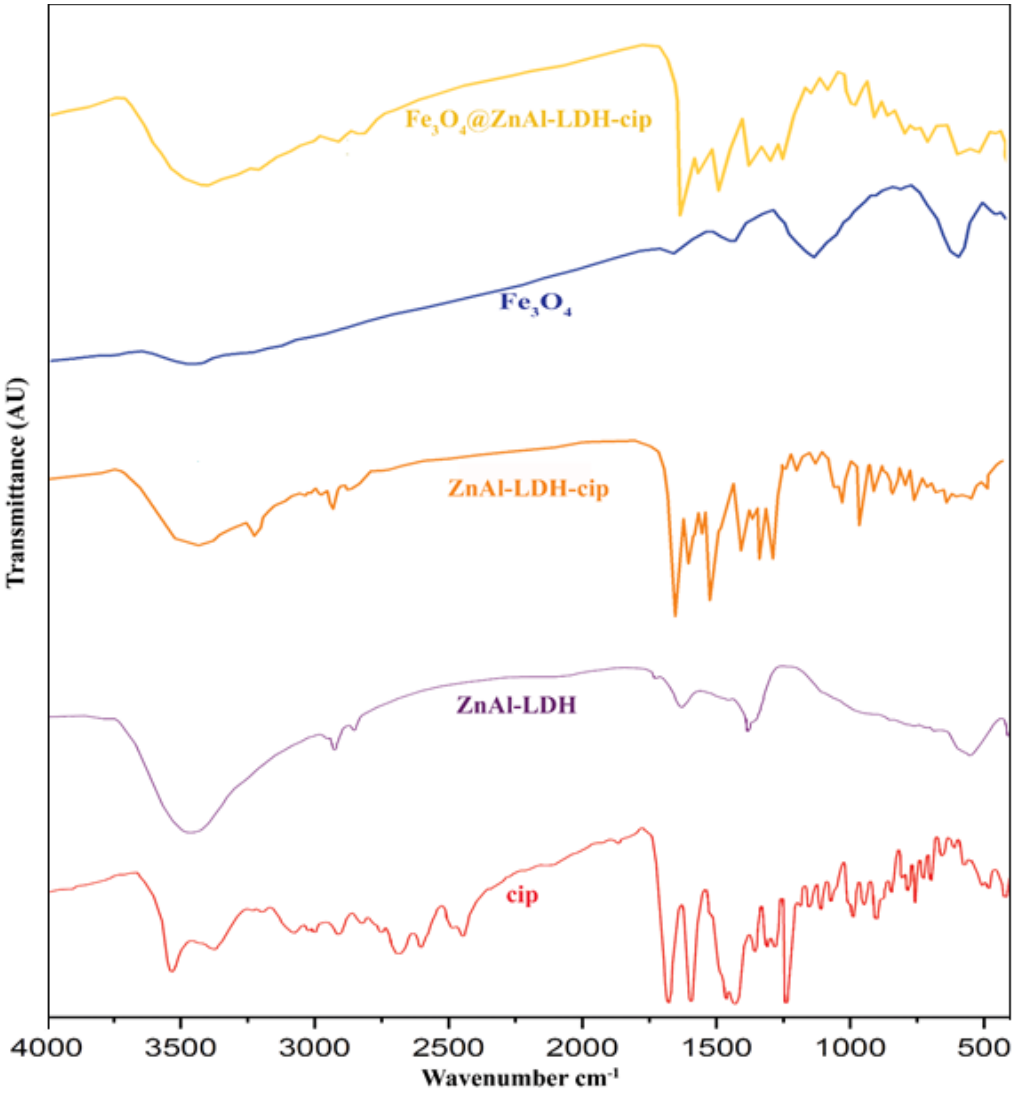


Fig. 1. FT-IR spectra of the pure ciprofloxacin, and the as-synthesized ZnAl-LDH, ZnAl-LDH-cip, $Fe_3O_4$ and $Fe_3O_4$@ZnAl-LDH-cip.

related $\lambda_{max}$ for cip, 275 nm. Then, the untrapped amount of the drug was determined based on the standard absorbance curve, plotted as the absorbance versus concentration for the different standard solutions of drug at the aforementioned wavelength. Finally, the drug-loading capacity was calculated by subtracting the amount of untrapped drug from the its initial amount [32]. On this basis, excellent loading capacities of ZnAl-LDH and $Fe_3O_4$@ZnAl-LDH were estimated as 95.87 % and 94.48 % for the intercalation of cip, respectively.

## RESULTS AND DISCUSSION

### *Analyses and characterizations*

FT-IR analysis was performed to confirm the formation of ZnAl-LDH and $Fe_3O_4$@ZnAl-LDH, and the loading of drug molecules on them leading to the ZnAl-LDH-cip, and also $Fe_3O_4$@

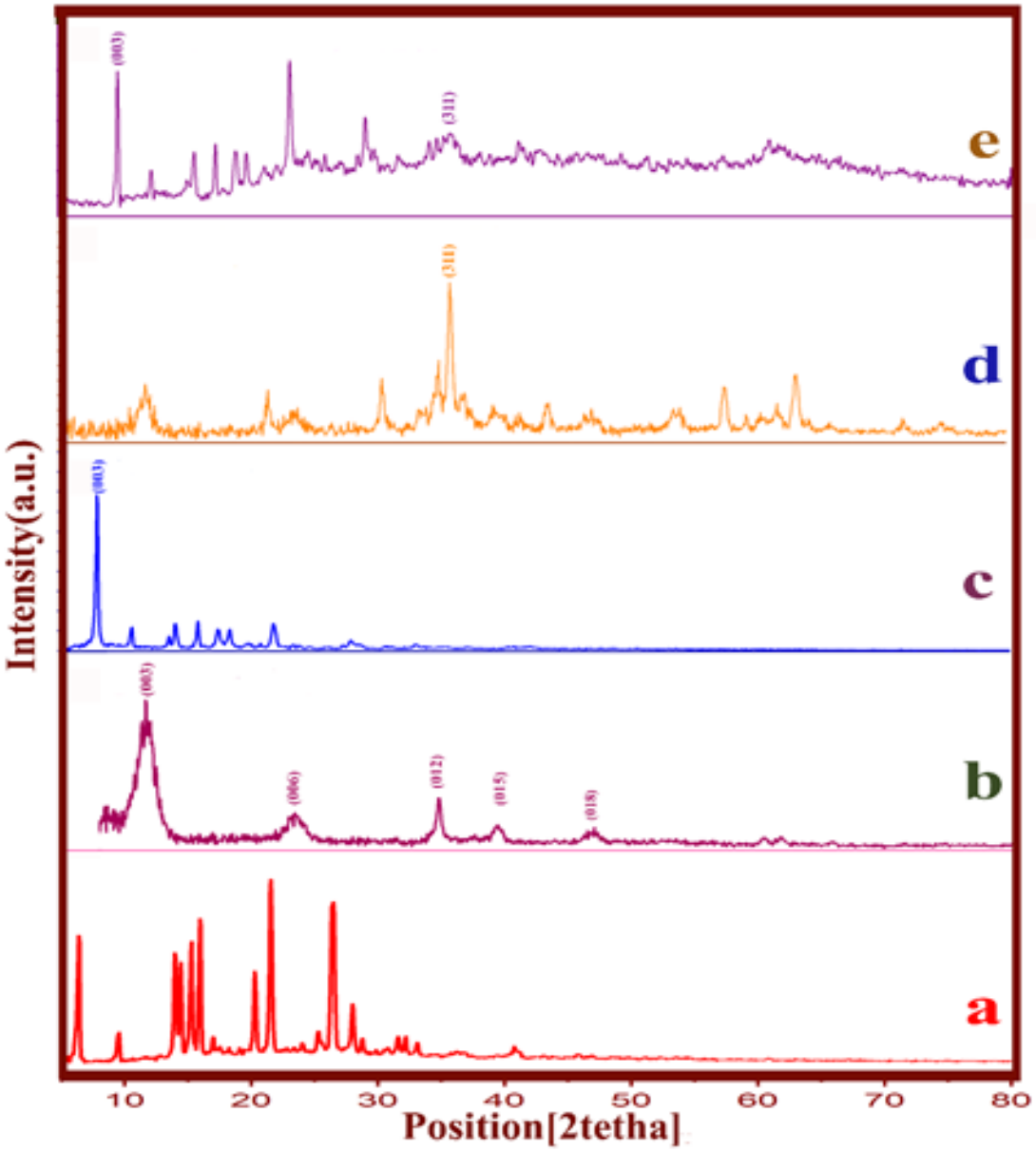


Fig. 2. XRD patterns of the pure ciprofloxacin (a), and the as-made ZnAl-LDH (b), ZnAl-LDH-cip (c), $Fe_3O_4$ (d) and $Fe_3O_4$@ZnAl-LDH-cip (e).

ZnAl-LDH-cip nanohybrid (Fig. 1). For the $Fe_3O_4$ sample, the absorption frequency at 594 $cm^{-1}$ was ascribed to the stretching vibration of Fe-O. As seen in the FT-IR spectrum of the as-synthesized ZnAl-LDH, the strong band recorded at around the wavenumber of 3452 $cm^{-1}$ is related to the stretching vibrations of the -OH group on the surface of layers or interlayer water molecules. In addition, the absorption band at about 1636 $cm^{-1}$ is related to the -OH bending vibrations of water molecules, and the band at 1383 $cm^{-1}$ represents the interlayer nitrate anions. The two absorption bands specific to LDH, which can be seen at wave numbers 526 and 426 $cm^{-1}$, are assigned to the stretching vibrations of the bonding of hydroxyl groups with zinc and aluminum [33].

The spectrum of ciprofloxacin shows many absorption bands due to the various vibrational modes of pure drugs including the aromatic rings, and carboxylic, phenyl, and pyrazine groups. The absorptions at 3085 and 2926 $cm^{-1}$ are related to the aromatic ring connected to the C-H bond. Also, the strong band appearing at 1707 $cm^{-1}$ belongs to the carboxylic acid group. The absorption band in the 1624 $cm^{-1}$ region belongs to the bond vibration of the phenyl group attached to COOH. The band at about 1270 $cm^{-1}$ corresponds to the vibration of the C-F bond. Besides, the absorption bands in the wave numbers ranges of 1280-1400 $cm^{-1}$ and 1610-1550 $cm^{-1}$ are characteristic of the symmetric and asymmetric vibrations of the O-C-O bond, respectively. The carboxylic acid group of ciprofloxacin loses its acidic H in the alkaline environment, and thus, it binds with LDH layers from its negative end and replaces the interlayer nitrate anion. In the cases of cip-loaded samples, as can be observed in Fig. 1, the appearance of vital absorption bands of the pristine LDH structure, magnetite core, and several characteristic vibrations of the bare

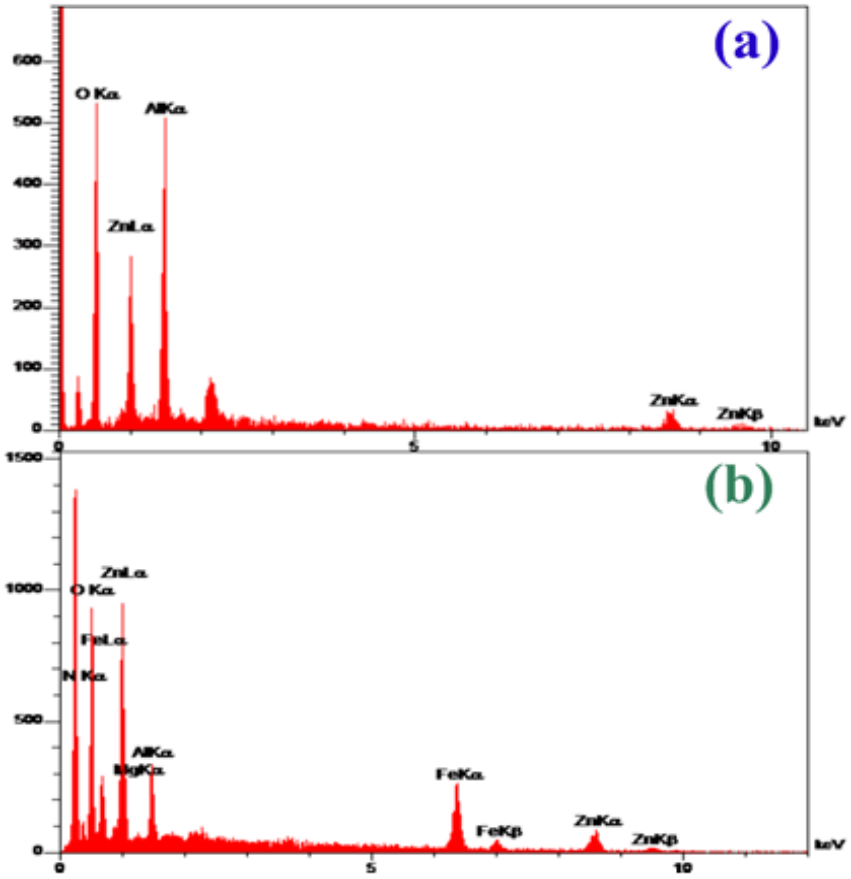


Fig. 3. EDX spectra of the as-produced ZnAl-LDH (a) and $Fe_3O_4$@ZnAl-LDH-cip (b).

drug clearly prove the successful loading of cip molecules and preparation of the ZnAl-LDH-cip and $Fe_3O_4$@ZnAl-LDH-cip. Also, the presence of absorption bands related to layered double hydroxide nanostructures and the structure of the drug is considered evidence of drug loading [34].

The XRD patterns of the pure drugs, as-prepared ZnAl-LDH and $Fe_3O_4$ samples, and the intercalated hybrid materials of ZnAl-LDH-cip and $Fe_3O_4$@ ZnAl-LDH-cip have been compared in Fig. 2(a-e). In the case of $Fe_3O_4$ (pattern 2d), the reflection peaks at 2θ = 30.20°, 35.52°, 43.13°, 57.20°, 62.52°, derived from the reflection planes of (220), (311), (400), (422), (511) and (440), respectively, indicate the good crystalline phase of magnetite with an inverse spinel structure, according to JCPDS card No. 19-0629. For ZnAl-LDH sample (Fig. 2b), the diffraction lines related to the (003), (006), (012), (015), and (018) crystal planes are located at 11.77 °, 23.41 °, 34.76 °, 39.36 °, and 46.86°, in agreement with the classical structure described in the literature (rhombohedral phase, space

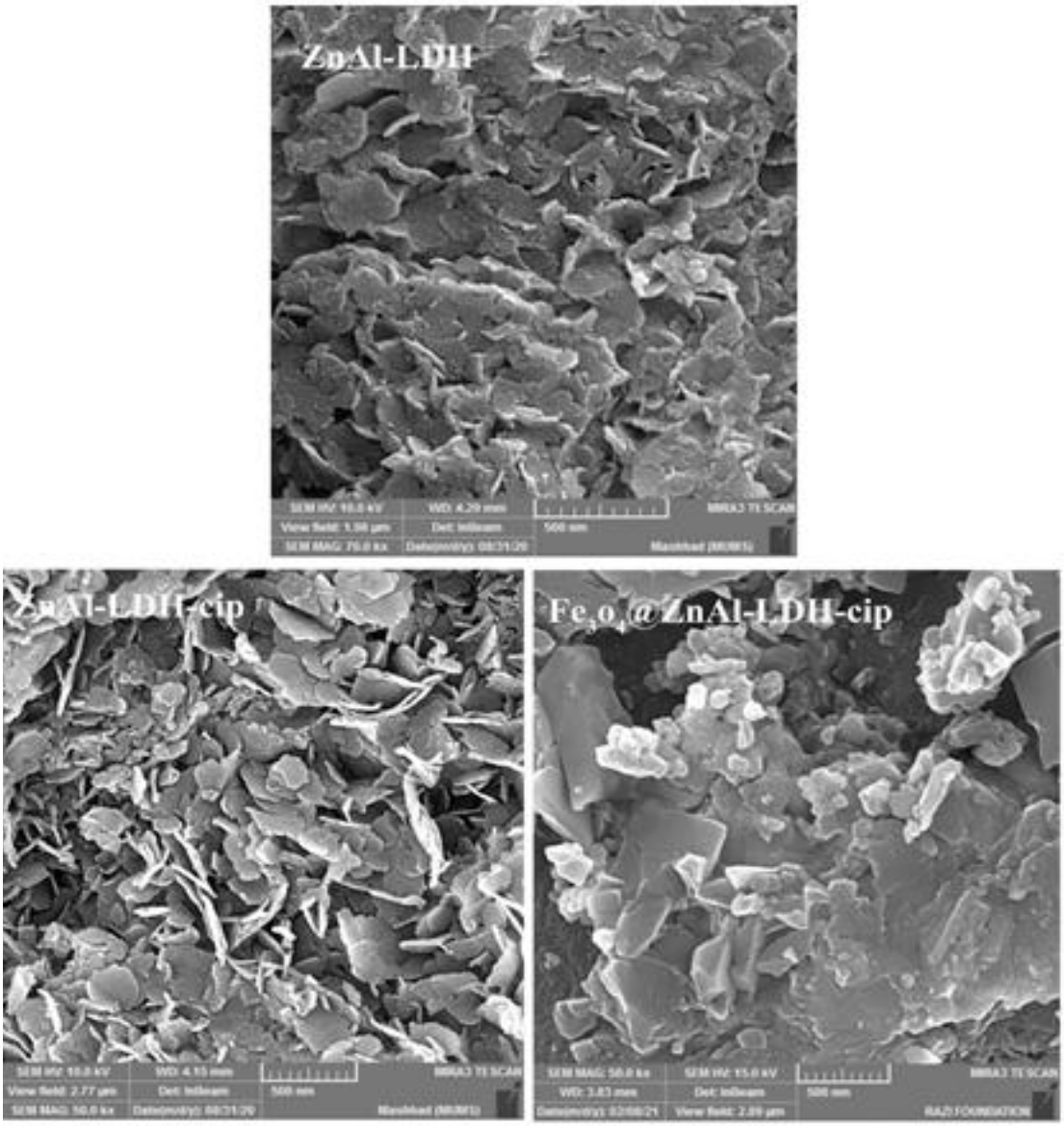


Fig. 4. FE-SEM images of the as-prepared nanostructures: ZnAl-LDH, ZnAl-LDH-cip and $Fe_3O_4$@ZnAl-LDH-cip.

group R-3m). The high intense and relatively narrow peak for the (003) plane illustrates the crystalline LDH [35, 36]. It can be noticed that the (003) reflection have been shifted to a lower angle (2θ) region (below 5°) after the cip intercalation, as seen in the 2(c, e) patterns. This displacement on the one hand and the lack of peaks relevent to the drug on the other exhibit that the nitrate ions are replaced with cip, and the basal spacing of layered materials is enlarged. Further, the presence of characteristic peak of $Fe_3O_4$, related to crystal plane (311), confirms the existence of a magnetite core [37, 38].

Besides, the chemical composition of products was studied using energy-dispersive spectroscopy. The peaks of Zn and Al as metallic cations of the as-made LDH, and that of Fe, related to the magnetite core in the case of $Fe_3O_4$@ZnAl-LDH-cip, are observed in Fig. 3. Also, the EDX spectra exhibit the presence of N and O as composing elements of the as-produced nanocomposites.

The morphology of the LDH samples was characterized by the FE-SEM microscopic imaging techniques, before and after cip-loading. As can be seen in Fig. 4, the ZnAl-LDH nanostructures illustrate a layered and plate-like morphology. However, in the case of ZnAl-LDH-cip, its morphology changes to the lumpy, because of the adsorption of some drug molecules on the surface of LDH during the loading process. According to SEM images, it is noticeable that the particles of $Fe_3O_4$@ZnAl-LDH-cip nanohybrid are the LDH sheets that are stuck together due to their magnetic properties.

The thermogravimetric (TG) curve of $Fe_3O_4$@ZnAl-LDH-cip reveals four stages (Fig. 5a). In the first, at about 50 to 150 °C, the water molecules placed in the layers lost. In the second stage, the dehydroxylation and in result, the loss of layered double hydroxide sheets happens at a temperature range of approximately 300-550 °C. A lot of heat is released during the thermal decomposition of the layers. In the following, we will face the destruction of ciprofloxacin drug molecules, which according to the evidence, the melting point of this drug is about 255 °C, while the thermal resistance of the drug increases by being placed in the plates of layered double hydroxide nanostructures. We continue to see the resistance and non-decomposition of the $Fe_3O_4$ structure with increasing temperature.

*In vitro drug release*

For studying the dissolution behavior and total drug release from ZnAl-LDH and $Fe_3O_4$@ZnAl-LDH materials, a 20 mg sample of the nanohybrid was added to 5 ml of the medium solution (phosphate-buffered saline, pH=7.4) in a dialysis bag. Then, the bag was suspended in 500 ml PBS at 37 °C, under constant and continuous stirring. A three-mililiter sample of the suspension was withdrawn and

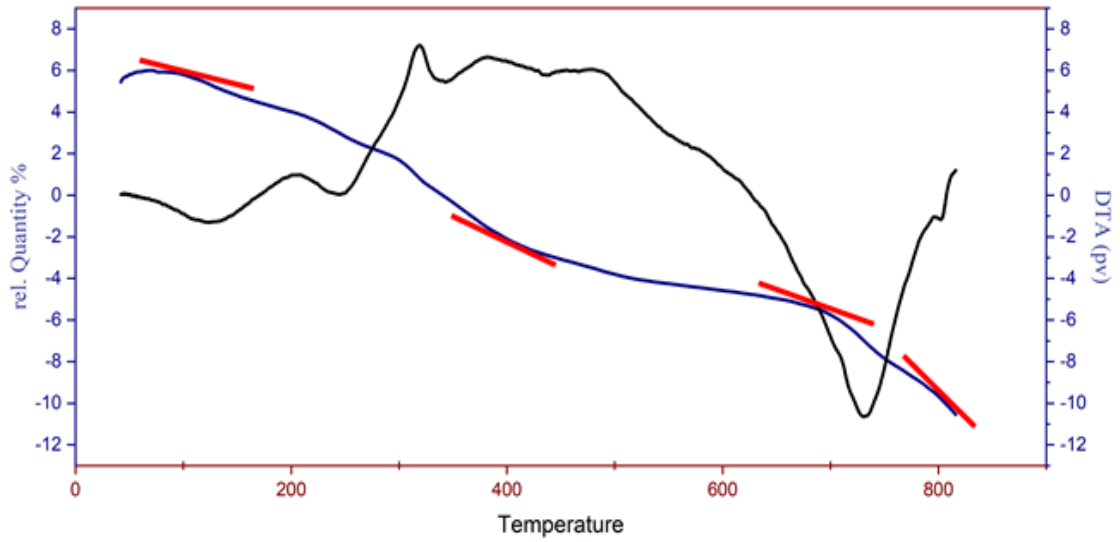


Fig. 5. TGA curves of the as-prepared $Fe_3O_4$@ZnAl-LDH-cip sample.

analyzed by UV-vis spectrophotometer at 275 nm, and in order to maintain the medium at constant volume, 3 ml of fresh PBS was added to the glass. The gradual release profile was measured for 24 hours until the concentration of the drug reached to stable level [39, 40]. The procedure was designed so that the drug concentration in fully released condition would not exceed 10 % of its solubility amount in the saturated solution, referred to as the 'sink conditions' [41]. According to the release profiles of drugs from the fabricated nanohybrid systems, given in Fig. 6, the high delivered amounts of 81.27 % and 82.43 % were found during 24 h for ZnAl-LDH-cip, and $Fe_3O_4$@ ZnAl-LDH-cip, respectively. On the other hand, a more remarkable rate, 82.24 %, at the releasing time of 6 h in the case of $Fe_3O_4$@ZnAl-LDH-cip, compared to that of ZnAl-LDH-cip, 75.03 %, indicates that the as-made $Fe_3O_4$@ZnAl-LDH can better play the role of a promising nanocarrier in the targeted and controlled drug delivery systems.

## CONCLUSION

In summary, ZnAl-LDH and $Fe_3O_4$@ZnAl-LDH were successfully synthesized through a novel co-precipitation method at moderate alkaline media derived from an ammonia atmosphere. Further, ciprofloxacin was intercalated in the interlayer spaces of the as-made LDH structures. The products' compositional structure, surface morphology, porosity, magnetic and thermostability properties were well characterized using various techniques. The increase in the space of interlayer in X-ray diffraction analysis indicated that the drugs were successfully intercalated into the LDH nanostructures (ZnAl-LDH-cip, 95.87 % and $Fe_3O_4$@ZnAl-LDH-cip, 94.48 %). Also, the surface morphology, examined by the scanning electron microscope images showed the stacked sheet of LDHs. In addition, the drug release properties were studied in PBS buffer (pH=7.4) at 37 °C and exhibited a sustained release profile. The great rates of 81.27 % and 82.43 % were found after 24 h for ZnAl-LDH-cip and $Fe_3O_4$@ZnAl-LDH-cip, respectively.

## ACKNOWLEDGMENTS

The authors are grateful to University of Kashan

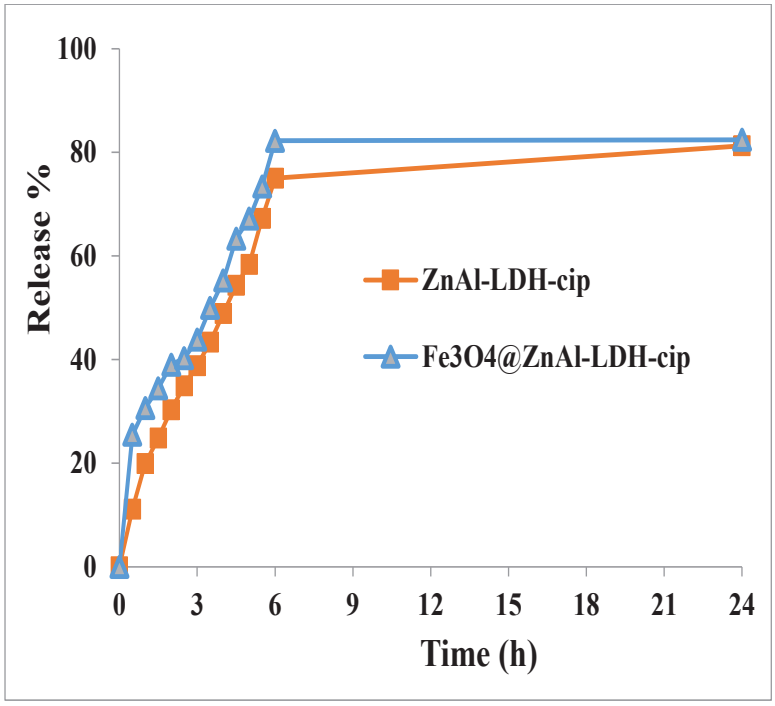


Fig. 6. Release profile of drug from ZnAl-LDH-cip and $Fe_3O_4$@ZnAl-LDH-cip nanohybrids.

for supporting this work by Grant No 785103/10.

## CONFLICT OF INTEREST

The authors declare that there is no conflict of interests regarding the publication of this manuscript.

## REFERENCES


1. de Sousa ALMD, dos Santos WM, de Souza ML, Silva LCPBB, Yun AEHK, Aguilera CSB, et al. Layered Double Hydroxides as Promising Excipients for Drug Delivery Purposes. European Journal of Pharmaceutical Sciences. 2021;165:105922.
2. Ameena Shirin VK, Sankar R, Johnson AP, Gangadharappa HV, Pramod K. Advanced drug delivery applications of layered double hydroxide. Journal of Controlled Release. 2021;330:398-426.
3. Xu C, Lu J, Zhou L, Liang J, Fang L, Cao F. Multifunctional nanocomposite eye drops of cyclodextrin complex@ layered double hydroxides for relay drug delivery to the posterior segment of the eye. Carbohydrate Polymers. 2021;260:117800.
4. Ebadi M, Buskaran K, Bullo S, Hussein MZ, Fakurazi S, Pastorin G. Drug delivery system based on magnetic iron oxide nanoparticles coated with (polyvinyl alcohol-zinc/aluminium-layered double hydroxide-sorafenib). Alexandria Engineering Journal. 2021;60(1):733-747.
5. Barkhordari S, Alizadeh A. Fabrication of pH-sensitive chitosan/layered double hydroxide (LDH)/ $Fe_3O_4$ nanocomposite hydrogel beads for controlled release of diclofenac. Polymer Bulletin. 2021;79(7):5533-5548.
6. Mallakpour S, Azadi E, Hussain CM. Recent advancements in synthesis and drug delivery utilization of polysaccharides-based nanocomposites: The important role of nanoparticles and layered double hydroxides. International Journal of Biological Macromolecules. 2021;193:183-204.
7. Hu T, Gu Z, Williams GR, Strimaite M, Zha J, Zhou Z, et al. Layered double hydroxide-based nanomaterials for biomedical applications. Chemical Society Reviews. 2022;51(14):6126-6176.
8. Jing G, Yang L, Wang H, Niu J, Li Y, Wang S. Interference of layered double hydroxide nanoparticles with pathways for biomedical applications. Advanced Drug Delivery Reviews. 2022;188:114451.
9. Younes HA, Khaled R, Mahmoud HM, Nassar HF, Abdelrahman MM, Abo El-Ela FI, et al. Computational and experimental studies on the efficient removal of diclofenac from water using ZnFe-layered double hydroxide as an environmentally benign absorbent. Journal of the Taiwan Institute of Chemical Engineers. 2019;102:297-311.
10. Tahsiri Z, Niakousari M, Hosseini SMH, Majdinasab M. Magnetic layered double hydroxide nanosheet as a biomolecular vessel for enzyme immobilization. International Journal of Biological Macromolecules. 2022;209:1422-1429.
11. Abo El-Reesh GY, Farghali AA, Taha M, Mahmoud RK. Novel synthesis of Ni/Fe layered double hydroxides using urea and glycerol and their enhanced adsorption behavior for Cr(VI) removal. Scientific Reports. 2020;10(1).
12. Sahoo DP, Das KK, Mansingh S, Sultana S, Parida K. Recent progress in first row transition metal Layered double hydroxide (LDH) based electrocatalysts towards water splitting: A review with insights on synthesis. Coordination Chemistry Reviews. 2022;469:214666.
13. Karim AV, Hassani A, Eghbali P, Nidheesh PV. Nanostructured modified layered double hydroxides (LDHs)-based catalysts: A review on synthesis, characterization, and applications in water remediation by advanced oxidation processes. Current Opinion in Solid State and Materials Science. 2022;26(1):100965.
14. Pires Figueiredo M, Borrego-Sánchez A, Pimentel C, Pérez de la Luz A, Viseras C, Sainz-Díaz CI. Experimental and Theoretical Studies on the Intercalation of Naproxen into the Mg2Al and Zn2Al Layered Double Hydroxides by Ion Exchange Reaction. Journal of Pharmaceutical Sciences. 2022;111(8):2369-2377.
15. Mourid EH, Lakraimi M, Legrouri A. Preparation of well-structured hybrid material through ion exchange of chloride by 2,4,5-trichlorophenoxyacetic herbicide in a layered double hydroxide. Materials Chemistry and Physics. 2022;278:125570.
16. Pavlovic M, Szerlauth A, Muráth S, Varga G, Szilagyi I. Surface modification of two-dimensional layered double hydroxide nanoparticles with biopolymers for biomedical applications. Advanced Drug Delivery Reviews. 2022;191:114590.
17. Zhang Z, Wells CJR, Liang R, Davies G-L, Williams GR. Gadolinium Doped Layered Double Hydroxides for Simultaneous Drug Delivery and Magnetic Resonance Imaging. Journal of Cluster Science. 2022;34(1):385-394.
18. Kankala RK. Nanoarchitectured two-dimensional layered double hydroxides-based nanocomposites for biomedical applications. Advanced Drug Delivery Reviews. 2022;186:114270.
19. Zhang L, Liang J, Yue L, Dong K, Li J, Zhao D, et al. Benzoate anions-intercalated NiFe-layered double hydroxide nanosheet array with enhanced stability for electrochemical seawater oxidation. Nano Research Energy. 2022;1:e9120028.
20. Sohrabi H, Dezhakam E, Khataee A, Nozohouri E, Majidi MR, Mohseni N, et al. Recent trends in layered double hydroxides based electrochemical and optical (bio)sensors for screening of emerging pharmaceutical compounds. Environmental Research. 2022;211:113068.
21. Zhang Y, Cao J, Li J, Yuan Z, Li D, Wang L, et al. Self-assembled Cobalt-doped NiMn-layered double hydroxide (LDH)/V2CT MXene hybrids for advanced aqueous electrochemical energy storage properties. Chemical Engineering Journal. 2022;430:132992.
22. Dutta N, Newar P, Narzary M, Maji TK. Preparation and characterization of biobased hybrid nanocomposite of Polyvinyl chloride/thermoplastic starch with Mg–Al layered double hydroxide and waste rice husk ash. Journal of Polymer Research. 2022;29(9).
23. Maggi L, Bruni G, Ferrara C, Puscalau C, Quinzeni I, Friuli V, et al. Zaltoprofen-layered double hydroxide hybrids to enhance zaltoprofen solubility and dissolution rate. Applied Clay Science. 2023;231:106723.
24. Dilmaghani A, Hosseini K, Tarhriz V, Yousefi V. Synthesis of Zeolitic imidazolate frameworks-8@ layered double hydroxide polyhedral nanocomposite with designed porous voids as an effective carrier for anti-cancer drug-controlled delivery. IET Nanobiotechnology. 2023;17(4):326-336.
25. Nwabuife JC, Omolo CA, Govender T. Nano delivery systems to the rescue of ciprofloxacin against resistant bacteria "E. coli; P. aeruginosa; Saureus; and MRSA" and their infections.

Journal of Controlled Release. 2022;349:338-353.
26. Zhang H, Quan H, Yin S, Sun L, Lu H. Unraveling the Toxicity Associated with Ciprofloxacin Biodegradation in Biological Wastewater Treatment. Environmental Science & Technology. 2022;56(22):15941-15952.
27. Wang X, Pan F, Xiang Z, Zeng Q, Pei K, Che R, et al. Magnetic vortex core-shell $Fe_3O_4$@C nanorings with enhanced microwave absorption performance. Carbon. 2020;157:130-139.
28. Yavuz E, Tokalıoğlu Ş, Patat Ş. Core–shell $Fe_3O_4$ polydopamine nanoparticles as sorbent for magnetic dispersive solid-phase extraction of copper from food samples. Food Chemistry. 2018;263:232-239.
29. Fischer S, Mehlenbacher RD, Lay A, Siefe C, Alivisatos AP, Dionne JA. Small Alkaline-Earth-based Core/Shell Nanoparticles for Efficient Upconversion. Nano Letters. 2019;19(6):3878-3885.
30. Yousefi V, Tarhriz V, Eyvazi S, Dilmaghani A. Synthesis and application of magnetic@layered double hydroxide as an anti-inflammatory drugs nanocarrier. Journal of Nanobiotechnology. 2020;18(1).
31. Basavaiah K, Pavankumar Y, Rao AVP. A facile one-step synthesis of PTSA-doped tetraaniline nanostructure/magnetite nanoparticles via self-assembly method. Journal of Nanostructure in Chemistry. 2013;3(1).
32. Shah AA, Kehinde EO, Patel J. An Emerging Era for Targeted Drug Delivery: Nanosponges. Journal of Pharmaceutical Research International. 2021:153-160.
33. Lu Z-H, Abdelhai Senosy I, Zhou D-D, Yang Z-H, Guo H-M, Liu X. Synthesis and adsorption properties investigation of $Fe_3O_4$@ZnAl-LDH@MIL-53(Al) for azole fungicides removal from environmental water. Separation and Purification Technology. 2021;276:119282.
34. Cherif NF, Constantino VRL, Hamdaoui O, Leroux F, Taviot-Guého C. New insights into two ciprofloxacin-intercalated arrangements for layered double hydroxide carrier materials. New Journal of Chemistry. 2020;44(24):10076-10086.
35. Li W, Liu A, Tian H, Wang D. Controlled Release of Nitrate and Molybdate Intercalated in Zn-Al-Layered Double Hydroxide Nanocontainers towards Marine Anticorrosion Applications. Colloid and Interface Science Communications. 2018;24:18-23.
36. Iqbal MA, Secchi M, Iqbal MA, Montagna M, Zanella C, Fedel M. MgAl-LDH/graphene protective film: Insight into LDH-graphene interaction. Surface and Coatings Technology. 2020;401:126253.
37. Ni J, Xue J, Xie L, Shen J, He G, Chen H. Construction of magnetically separable NiAl LDH/ $Fe_3O_4$–RGO nanocomposites with enhanced photocatalytic performance under visible light. Physical Chemistry Chemical Physics. 2018;20(1):414-421.
38. Salguero Y, Valenti L, Rojas R, García MC. Ciprofloxacin-intercalated layered double hydroxide-in-hybrid films as composite dressings for controlled antimicrobial topical delivery. Materials Science and Engineering: C. 2020;111:110859.
39. Chai J, Ma Y, Guo T, He Y, Wang G, Si F, et al. Assembled $Fe_3O_4$ nanoparticles on Zn Al LDH nanosheets as a biocompatible drug delivery vehicle for pH-responsive drug release and enhanced anticancer activity. Applied Clay Science. 2022;228:106630.
40. Pooresmaeil M, Namazi H. Facile coating of the methotrexate-layered double hydroxide nanohybrid via carboxymethyl starch as a pH-responsive biopolymer to improve its performance for colon-specific therapy. European Polymer Journal. 2022;165:111026.
41. Korzeniowska A, Strzempek W, Makowski W, Menaszek E, Roth WJ, Gil B. Incorporation and release of a model drug, ciprofloxacin, from non-modified SBA-15 molecular sieves with different pore sizes. Microporous and Mesoporous Materials. 2020;294:109903.